Structural Polymorphism Kinetics Promoted by Charged Oxygen Vacancies in HfO_2

Li-Yang Ma[1,2] and Shi Liu[2,3,*]
[1]*Fudan University, Shanghai 200433, China*
[2]*Key Laboratory for Quantum Materials of Zhejiang Province, Department of Physics, School of Science, Westlake University, Hangzhou, Zhejiang 310024, China*
[3]*Institute of Natural Sciences, Westlake Institute for Advanced Study, Hangzhou, Zhejiang 310024, China*

(Received 20 April 2022; revised 9 August 2022; accepted 24 January 2023; published 27 February 2023)

Defects such as oxygen vacancy are widely considered to be critical for the performance of ferroelectric HfO_2-based devices, and yet atomistic mechanisms underlying various exotic effects such as wake-up and fluid imprint remain elusive. Here, guided by a lattice-mode-matching criterion, we systematically study the phase transitions between different polymorphs of hafnia under the influences of neutral and positively charged oxygen vacancies using a first-principles-based variable-cell nudged elastic band technique. We find that the positively charged oxygen vacancy can promote the transition of various nonpolar phases to the polar phase kinetically, enabled by a transient high-energy tetragonal phase and extreme charge-carrier-inert ferroelectricity of the polar $Pca2_1$ phase. The intricate coupling between structural polymorphism kinetics and the charge state of the oxygen vacancy has important implications for the origin of ferroelectricity in HfO_2-based thin films as well as wake-up, fluid imprint, and inertial switching.

DOI: 10.1103/PhysRevLett.130.096801

Ferroelectric memory has long been considered as a competitive non-volatile information storage technology because of various merits such as fast switching rate, low power consumption, and high endurance [1–3]. Conventional perovskite ferroelectrics are not compatible with the modern complementary metal oxide semiconductor (CMOS) technology, severely limiting the scalability [4]. The discovery of ferroelectricity in silicon-doped thin films of hafnium oxide in 2011 [5] quickly made HfO_2 a leading candidate material for incorporating ferroelectric functionalities into integrated circuits. Thanks to its robust electric dipoles at the nanoscale [6], simple composition, and the CMOS compatibility, HfO_2-based ferroelectrics have already been implemented in several memory devices [7,8].

The commercialization of ferroelectric HfO_2-based devices is mainly hindered by the device reliability issues associated with the profound wake-up effect, strong imprint, and limited endurance [9,10]. For example, the imprint effect, manifested as the shift of a hysteresis loop along the voltage axis with time, will destabilize one of the polarization states and cause retention loss [11]. It is widely accepted that the polar orthorhombic (PO) $Pca2_1$ phase of HfO_2 is responsible for the ferroelectricity [12–16], despite being higher in energy than the nonpolar monoclinic (M) $P2_1/c$ phase. The stabilization of the PO phase in thin films has been attributed to the concerted effects of extrinsic factors such as surface or interface effects of grains [12,16–20], clamping stress [21–23], defects [24–30], and electric fields [22]. The as-prepared HfO_2-based thin film often contains high volume factions of nonpolar M phase and tetragonal (T) $P4_2/nmc$ phase [26,31,32]. The models explaining the performance instability during electrical cycling can be categorized into two groups: (i) defects and their evolution; (ii) electric field-induced structural polymorphism that may originate from defects [33]. In this Letter, we discover an intricate coupling between structural polymorphism kinetics and the charge state of the oxygen vacancy in HfO_2 that has important implications for the origin of ferroelectricity and several device reliability issues.

We start by emphasizing two unique features of the ferroelectric PO phase of HfO_2. First, the X_2^- lattice mode characterized by antiparallel x displacements of neighboring oxygen atoms [Fig. 1(a)] plays an important role in structural polymorphism of HfO_2. Though phase transitions between different polymorphs of HfO_2 have been investigated with density functional theory (DFT) calculations previously [23], the importance of the X_2^- mode matching was not appreciated. There exist multiple pathways connecting two phases depending on the choice of atom-to-atom mapping. We find that an atomic mapping that conserves the sign of the X_2^- mode gives a lower enthalpy barrier than a mapping that reverses the X_2^- mode. As shown in Fig. 1(a), the X_2^--sign-conserving pathway of $T \rightarrow$ PO has an enthalpy barrier of 2.5 meV per formula unit (f.u.), much lower than the pathway with the X_2^- mode reversed (47.5 meV/f.u.). Recent DFT studies also found that the polarization switching in PO that reverses the X_2^- mode needs to overcome a large barrier [34]. The small

 © 2023 American Physical Society

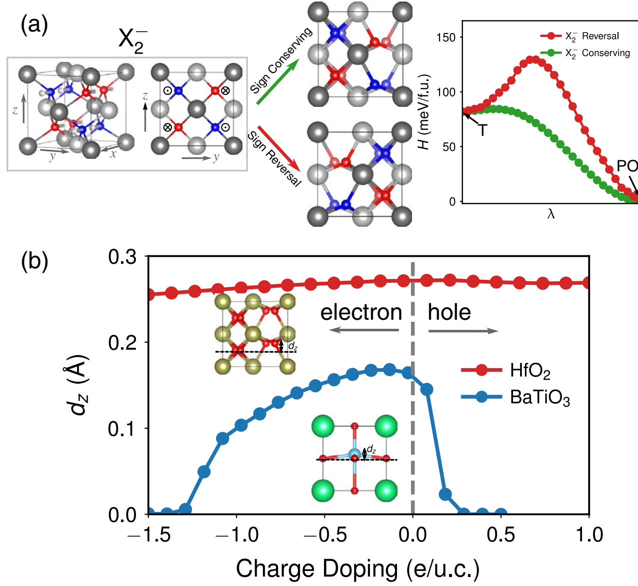

FIG. 1. (a) Schematic illustration of the X_2^- mode in the tetragonal phase of HfO_2. The tetragonal unit cell has the long axis along x. The closer and further Hf atoms are colored in dark and light gray; outward and inward displaced oxygen atoms are colored in blue and red, respectively. The generic phase space coordinate is denoted as λ. (b) Polar atomic displacement (d_z) as a function of charge-carrier concentration for the PO phase of HfO_2 and tetragonal $BaTiO_3$. The insets illustrate the definitions of d_z in HfO_2 and $BaTiO_3$.

enthalpy barrier of $T \to$ PO already hints at the importance of nonpolar-polar structural polymorphism in HfO_2-based devices.

Another intriguing feature is the extreme charge-carrier-inert ferroelectricity of the PO phase. We compute the polar atomic displacements in ferroelectric tetragonal $BaTiO_3$ and the PO phase of HfO_2 as a function of charge-carrier concentration obtained via the background-charge method [35]. Both hole doping and electron doping quickly suppress the polar displacements in tetragonal $BaTiO_3$ [36]. In contrast, the local atomic displacements of polar oxygen atoms in PO are insensitive to charge-carrier doping [Fig. 1(b)]. Such feature, likely resulting from the improper nature of ferroelectric HfO_2 [37], suggests that the PO phase can support a substantial amount of charged defects while maintaining the polar structure. Since the charge injection to and entrapment from defects occur frequently during the electrical cycling, understanding the impacts of charged defects on polymorphism kinetics is expectedly important.

Here, we focus on neutral oxygen vacancy (V_O^0) and doubly positively charged oxygen vacancy (V_O^{2+}), as they are known prominent defects in HfO_2-based thin films [33,38], particularly at the electrode-HfO_2 interface [39–41]. Different from several previous DFT studies on oxygen-deficient HfO_2 where the assumed vacancy concentration reaches a rather high level (up to 12.5 f.u.% [42]), we focus on a relatively low vacancy concentration (3.125 f.u.%). DFT calculations are performed using Vienna *ab initio* simulation package (VASP) with Perdew-Burke-Ernzerhof (PBE) density functional [43]. Structural parameters of unit cells of hafnia polymorphs are optimized using a plane-wave cutoff of 600 eV, a $4 \times 4 \times 4$ Monkhorst-Pack k-point grid for Brillouin zone sampling, an energy convergence threshold of 10^{-6} eV, and a force convergence threshold of 10^{-3} eV/Å. All possible configurations of a 48-atom supercell with an oxygen vacancy concentration of 3.125 f.u.% are explored to identify the lowest-energy configuration. The minimum energy pathway (MEP) connecting two polymorphs is identified with the variable-cell nudged elastic band (VCNEB) technique implemented in the USPEX code [44–46]. The main difference between conventional NEB and VCNEB is that VCNEB allows lattice constants to change during solid-solid transformations, thus capable of quantifying the intrinsic transition barrier between two phases possessing different lattice constants. It is noted that lattice constants and phase transition barriers predicted with PBE are comparable with values computed with SCAN [47]. More computational details are reported in Supplemental Material [48] that includes Refs. [11,23,49–68].

We first examine the intrinsic transition barriers in the absence of defects between different phases of HfO_2 including an "antiferroelectric-like" orthorhombic (AO) $Pbca$ phase and another polar orthorhombic $Pmn2_1$ phase that may form in (111)-oriented $Hf_{0.5}Zr_{0.5}O_2$ thin films [69,70]. All pathways conserve the sign of the X_2^- mode (Fig. S1 in [48]). Taking the lowest-energy M phase as the reference, the energy of T, AO, PO, and $Pmn2_1$ phase is 166, 73, 84, and 143 meV/f.u., respectively. The transitions of $T \to M$, $T \to$ PO, and $T \to Pmn2_1$ are all kinetically fast with negligible enthalpy barriers (< 5 meV/f.u., 2(a)), indicating the precursor role of the high-temperature T phase [23]. The transition of $T \to$ AO needs to overcome a large kinetic barrier despite AO being the second most favored phase thermodynamically. The transitions from the polar $Pmn2_1$ phase to M and $Pca2_1$ only needs to overcome a small barrier of 28 and 37 meV/f.u., respectively. We suggest that although the emergence of the $Pmn2_1$ phase from the T phase is effortless kinetically, it may quickly evolve to other phases such that its transient presence during crystallization is probably undetectable in experiments.

Phase transitions of $Pca2_1$ to other nonpolar phases are all hindered by large barriers. Overall, the formation of the M phase is the most favored process both kinetically and thermodynamically in the absence of extrinsic effects. This explains why the most stable M phase dominates in bulk synthesis. We discover that $M \to$ PO involves another lattice mode, X_5^y. It is impossible for the transition pathway to conserve both X_5^y and X_2^-, thus making $M \to$ PO a high-barrier (169 meV/f.u.) process that cannot be activated by

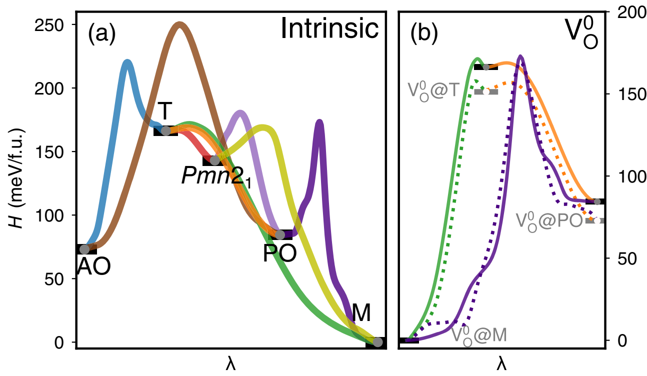

FIG. 2. (a) Minimum energy pathways connecting different polymorphs of HfO_2 obtained with VCNEB. (b) Comparison of transition pathways between M, T, and PO phases at the pristine state (solid lines) and those in the presence of V_O^0 at a concentration of 3.125% (dashed lines). The energy of the M phase is chosen as the energy zero point.

an electric field alone (see Sec. I.C in Supplemental Material [48]). This is inconsistent with experimental observations that a substantial amount of M phase is transformed to the PO phase in the woken-up thin films of HfO_2 [15,50,64]. As we will discuss in below, the presence of charged oxygen vacancies resolves this puzzle.

The oxygen vacancy has long been postulated to be important for the stabilization of the PO phase. Experimentally, a low oxygen content during the deposition favors the formation of T and PO phases whereas a high oxygen content tends to stabilize the M phase [71,72]. However, DFT calculations suggested that even at a high V_O^0 concentration of ≈12.5 f.u.%, the M phase remains much more stable thermodynamically than the PO phase [73]. Rushchanskii *et al.* proposed that configurations with two-dimensional extended oxygen vacancies tend to transform into the PO phase [42], but the V_O^0 concentration in their model reached 12.5 f.u.%, much higher than typical experimental values of 2–3 f.u.% [30,72]. We further investigate the effects of V_O^0 on polymorphism kinetics at a concentration of 3.125 f.u.%. Compared with intrinsic defect-free cases, the presence of V_O^0 has little impact on the relative stability, nor does it substantially affect the kinetics of phase transitions [Fig. 2(b)]. We conclude that at experimentally relevant concentrations, V_O^0 alone cannot explain the strong impacts of O_2 partial pressures on the ferroelectric properties of HfO_2-based thin films.

Recently, He *et al.* reported that the presence of V_O^{2+} beyond some critical concentration will make PO more stable than M [67]. At a low V_O^{2+} concentration of 3.125 f.u.% studied here, we carefully examine the energetics of different configurations containing V_O^{2+} and find that M remains to be most stable thermodynamically (See Table S2 in Supplemental Material [48]). Interestingly, the

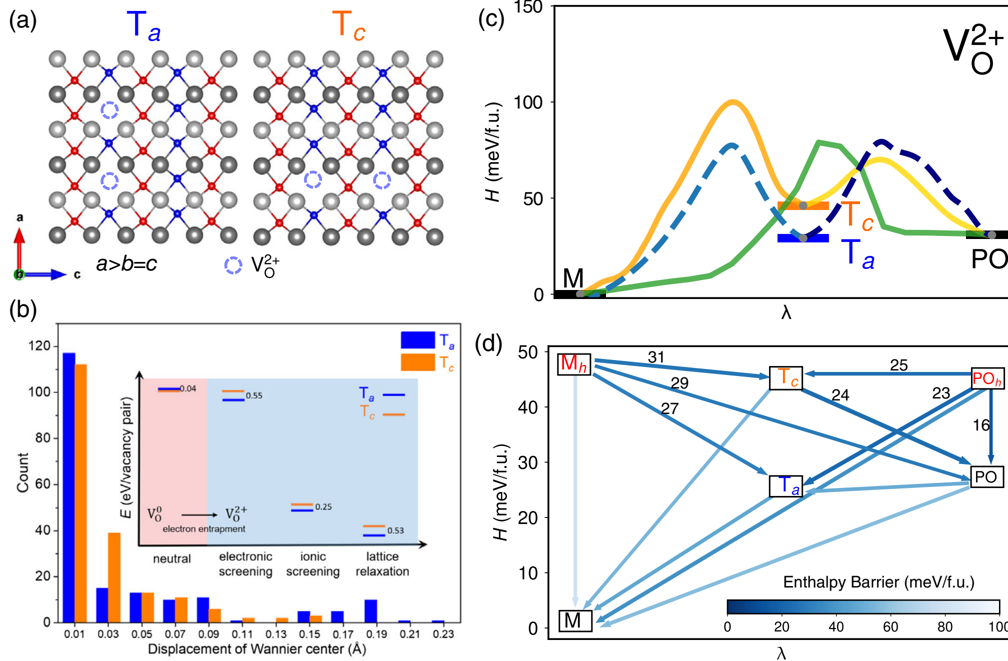

FIG. 3. (a) Schematics of two different configurations of the T phase containing a pair of V_O^{2+}. (b) Histograms of displacements of Wannier centers in T_a and T_c right after the electron entrapment of $V_O^0 \rightarrow V_O^{2+}$. The inset shows different contributions to the change in the relative stability between T_a and T_c. Only the energies of configurations containing the same type of oxygen vacancy are comparable. (c) Transition pathways in the presence of V_O^{2+} at a concentration of 3.125%. (d) Phase transition network involving multiple polymorphs of HfO_2 containing V_O^{2+}. The color of the arrow scales with the magnitude of the transition barrier (see values in Table S5 [48]).

relative stability between two representative configurations of the T phase, denoted as T_a and T_c [Fig. 3(a)], depends sensitively on the charge state of oxygen vacancy. Specifically, T_a and T_c has the vacancy pair aligned along the long axis a and the short axis c, respectively. Such local oxygen vacancy ordering is almost inevitable statistically even at a low vacancy concentration (see Sec. I.E and experimental evidences in Sec. III of Supplemental Material [48]). The energies of $V_O^0@T_a$ and $V_O^0@T_c$ are comparable when the oxygen vacancy is charge neutral, but $V_O^{2+}@T_c$ becomes rather unstable relative to $V_O^{2+}@T_a$ after the electron entrapment of $V_O^0 \rightarrow V_O^{2+}$. The strong impact of V_O^{2+} on the relative stability is confirmed with both 96-atom and 768-atom supercells (Table S3 [48]). We perform a series of calculations to identify and separate the contributions to the change in the relative stability (see Sec. IV of Supplemental Material [48]). As shown in Fig. 3(b), the electronic screening already makes $V_O^{2+}@T_a$ containing V_O^{2+} more stable than $V_O^{2+}@T_c$ by 0.55 eV. We compute the displacements of all Wannier centers (WCs, roughly viewed as the positions of electrons, Fig. S8 [48]) after $V_O^0 \rightarrow V_O^{2+}$. The displacements of some WCs in T_a are much larger than those in T_c, indicating a more substantial electronic charge density redistribution in T_a. The most displaced WC in $V_O^{2+}@T_a$ is of Hf-5p character (Fig. S9 [48]). After incorporating the effects of ionic screening and lattice relaxation, $V_O^{2+}@T_a$ containing V_O^{2+} remains more stable than $V_O^{2+}@T_c$ by 0.53 eV.

The MEPs connecting $V_O^{2+}@T_a$ ($V_O^{2+}@T_c$) to the most stable configurations of M and PO phases containing V_O^{2+} are shown in Fig. 3(c). We find that $V_O^{2+}@T_c \rightarrow V_O^{2+}@\mathrm{PO}$ with a barrier of 24 meV/f.u. is kinetically favored over $V_O^{2+}@T_c \rightarrow V_O^{2+}@M$ with a barrier of 54 meV/f.u., while M and PO remain well separated by a large barrier. Therefore, V_O^{2+} promotes $T_c \rightarrow \mathrm{PO}$ but suppresses $T_c \rightarrow M$. As T_a is more difficult to undergo phase transitions [Fig. 3(c)], it also explains why as-prepared thin films of HfO_2 often exhibit a high volume fraction of nonpolar T phase.

The V_O^{2+}-promoted nonpolar-polar structural polymorphism, $T_c \rightarrow \mathrm{PO}$, likely plays an important role for the emergence of ferroelectricity. A capping electrode was often required to induce the ferroelectricity in Si-doped HfO_2 thin films [74,75]. This could be due to the easy formation of V_O^{2+} at the metal/HfO_2 interface as the two electrons of V_O^0 may fall to the metal Fermi level [39]. Since raising the temperature effectively increases the charge-carrier concentration, we propose that during the high-temperature annealing treatment of thin films, the formation of V_O^{2+} at the metal-HfO_2 interface is facilitated such that the occurrence of $T_c \rightarrow \mathrm{PO}$ becomes substantial. Recent observations that the light ion bombardment can greatly enhance the ferroelectricity in HfO_2-based thin films [62] corroborates the V_O^{2+}-promoted formation of polar HfO_2. The difficulty to obtain the PO phase of HfO_2 through bulk synthesis may be attributed to the high formation energy of oxygen vacancy in bulk HfO_2 (6.38 eV) [76]. Moreover, the necessity of V_O^{2+} for $T_c \rightarrow$ PO is consistent with a large body of experimental data that nearly all cation dopants inducing ferroelectricity in HfO_2-based thin films are of p type because the substitution of Hf^{4+} with acceptor dopants such as Y^{3+} naturally promotes the formation of V_O^{2+} to maintain charge neutrality. The latest verification of intrinsic ferroelectricity in yttrium-doped HfO_2 thin films with a large remnant polarization of 64 $\mu C/cm^2$ [77] serves as another example supporting our hypothesis. For the same reason, the emergence of ferroelectricity in nitrogen-doped HfO_2 [29] could be arising from V_O^{2+} that compensates N_O^- [78].

The finding that V_O^{2+} can strongly modulate the relative configurational stability is not unique to the T phase. We discover an oxygen-deficient configuration of M (denoted as M_h) which is stable with V_O^0 but becomes highly unstable upon the charge entrapment from V_O^0. It is kinetically feasible for $V_O^{2+}@M_h$ to transform to $V_O^{2+}@T_c/T_a$ and $V_O^{2+}@\mathrm{PO}$ (< 29 meV/f.u.), highlighting that V_O^{2+} can enable a previously forbidden transition of $M \rightarrow \mathrm{PO}$. We also identify a configuration of PO, denoted as PO_h, which is destabilized by V_O^{2+} and easily transforms to nonpolar T and M phases. Contributions to the destabilization effect of V_O^{2+} are separated and quantified for M_h and PO_h, revealing a subtle competition between the electronic or ionic screening and lattice relaxation (see Sec. IV of the Supplemental Material [48]). The phase transition network involving multiple polymorphs containing V_O^{2+} [Fig. 3(d)] reveals that V_O^{2+} can enable facile transitions among nopolar M and T phases and the polar PO phase, the kinetic barriers of which are lower than the polarization switching barrier of the PO phase (≈55 meV/f.u.). We suggest that the charge state of V_O is another tuning knob to modulate the stabilities among competing phases in addition to epitaxial strain and electric boundary condition in modern thin-film technology [79].

The intricate coupling between V_O^{2+} and structural polymorphism kinetics could contribute to performance instability issues including wake-up and imprint. In a pristine HfO_2-based capacitor at room temperatures, V_O^0 is the dominant type of oxygen vacancy, as supported by recent DFT calculations [80] and experiments [40]. Therefore, V_O^0 may distribute at the metal-ferroelectric interface in the matrix of M, T, and PO phases [Fig. 4(a)]. Upon the application of a voltage, electrons of V_O^0 tend to detrap to the adjacent electrode [top electrode in Fig. 4(b)], leading to the formation of V_O^{2+} and the activation of $M_h \rightarrow \mathrm{PO}$ and $T_c \rightarrow \mathrm{PO}$ [Fig. 4(c)]. The diffusion of V_O^{2+}, recently observed in experiments [68],

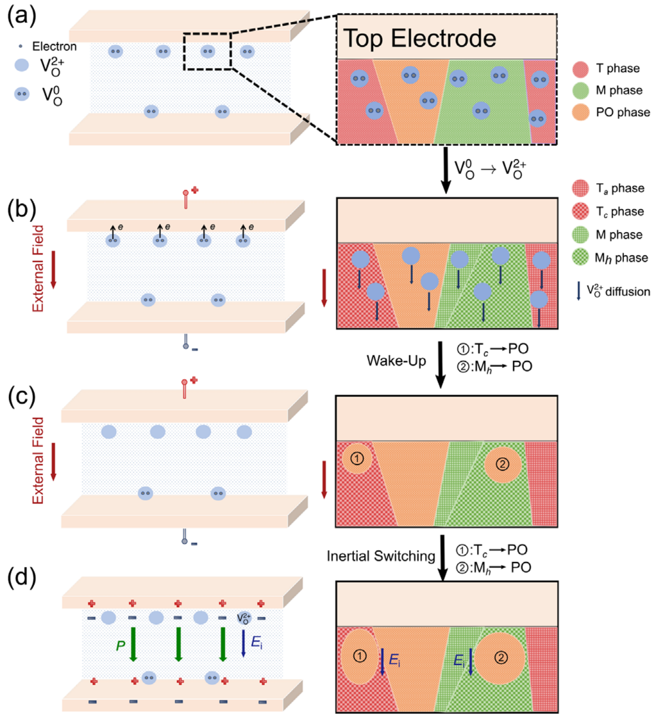

FIG. 4. Schematics of wake-up and inertial switching enabled by V_O^{2+}-promoted nonpolar-polar structural polymorphisms. Oxygen vacancies in the right schematics are not shown in (c) and (d) for clarity.

further helps the nonpolar-polar phase transitions in regions away from the electrode. Similar processes will occur near another electrode after reversing the bias. The overall result is a reduction of M and T and an increase of PO after field cycling, leading to the wake-up effect [64].

Finally, $M_h \rightarrow$ PO and $T_c \rightarrow$ PO to some extent explains "fluid imprint" in ferroelectric La-doped HfO_2 capacitors where the imprint is easily changeable and has a strong dependence on the switching prehistory [11]. As illustrated in Fig. 4(d), after the application of a preset pulse that polarize a woken-up capacitor (that still has residual nonpolar phases), the electron entrapment occurs more easily near the negative bound charge side. The presence of V_O^{2+} creates a local electric field that aligns with the bulk polarization, a probable source of imprint field (E_i). Even in the absence of additional bias, the V_O^{2+}-promoted nonpolar-polar phase transitions, due to their low kinetic barriers (< 29 meV/f.u.), could still occur driven by E_i, leading to continued polarization switching toward the same direction as the previously applied field, a feature of "inertial switching" [11]. The fluid imprint is associated with an evolving microstructure with a changing volume fraction of the PO phase.

In summary, the robust ferroelectricity of the $Pca2_1$ phase against charge doping highlights the necessity of understanding the effects of charged defects on the ferroelectric properties of HfO_2-based devices. Our DFT calculations suggest that the positively charged oxygen vacancy can drastically modulate the relative configurational stability of the same phase. The V_O^{2+}-promoted nonpolar-polar structural polymorphism is probably an overlooked yet important mechanism for the emergence of polar $Pca2_1$ phase in HfO_2-based thin films, offering a new perspective to experimentally observed electrode and doping effects. Generic mechanisms based on the coupling between V_O^{2+} and structural polymorphism kinetics are proposed to explain performance instability issues. To fully understand the wake-up and imprint effects, continued experimental and theoretical efforts are needed. Future studies focusing on the coupling between structural polymorphism kinetics and other extrinsic effects such as strain and direct experimental characterizations of these mechanisms are important for comprehending this complicated ferroelectric compound.

L. M. and S. L. acknowledge the supports from National Key R&D Program of China (2021YFA1202100), National Natural Science Foundation of China (12074319), and Westlake Education Foundation. The computational resource is provided by Westlake HPC Center. We thank Dr. Yichun Zhou and Jiangheng Yang for useful discussions inspired by which we discovered the importance of the X_2^- mode for phase transitions.

*liushi@westlake.edu.cn

[1] J. F. Scott, Applications of modern ferroelectrics, Science **315**, 954 (2007).

[2] W. Huang, W. Zhao, Z. Luo, Y. Yin, Y. Lin, C. Hou, B. Tian, C.-G. Duan, and X.-G. Li, A high-speed and low-power multistate memory based on multiferroic tunnel junctions, Adv. Electron. Mater. **4**, 1700560 (2018).

[3] T. Mikolajick, U. Schroeder, and S. Slesazeck, The past, the present, and the future of ferroelectric memories, IEEE Trans. Electron Devices **67**, 1434 (2020).

[4] C.-U. Pinnow and T. Mikolajick, Material aspects in emerging nonvolatile memories, J. Electrochem. Soc. **151**, K13 (2004).

[5] T. S. Böscke, J. Müller, D. Bräuhaus, U. Schröder, and U. Böttger, Ferroelectricity in hafnium oxide thin films, Appl. Phys. Lett. **99**, 102903 (2011).

[6] H.-J. Lee, M. Lee, K. Lee, J. Jo, H. Yang, Y. Kim, S. C. Chae, U. Waghmare, and J. H. Lee, Scale-free ferroelectricity induced by flat phonon bands in HfO_2, Science **369**, 1343 (2020).

[7] Q. Luo, Y. Cheng, J. Yang, R. Cao, H. Ma, Y. Yang, R. Huang, W. Wei, Y. Zheng, T. Gong, J. Yu, X. Xu, P. Yuan, X. Li, L. Tai, H. Yu, D. Shang, Q. Liu, B. Yu, Q. Ren, H. Lv, and M. Liu, A highly CMOS compatible hafnia-based ferroelectric diode, Nat. Commun. **11**, 1391 (2020).

[8] M.-K. Kim, I.-J. Kim, and J.-S. Lee, CMOS-compatible ferroelectric NAND flash memory for high-density, low-power, and high-speed three-dimensional memory, Sci. Adv. **7**, eabe1341 (2021).

[9] H. Mulaosmanovic, P. D. Lomenzo, U. Schroeder, S. Slesazeck, T. Mikolajick, and B. Max, Reliability aspects of ferroelectric hafnium oxide for application in non-volatile memories, *2021 IEEE International Reliability Physics Symposium (IRPS)* (IEEE, 2021), 10.1109/irps46558.2021.9405215.

[10] S. Mueller, J. Muller, U. Schroeder, and T. Mikolajick, Reliability characteristics of ferroelectric Si: HfO_2 thin films for memory applications, IEEE Trans. Electron Devices **13**, 93 (2013).

[11] P. Buragohain, A. Erickson, P. Kariuki, T. Mittmann, C. Richter, P. D. Lomenzo, H. Lu, T. Schenk, T. Mikolajick, U. Schroeder, and A. Gruverman, Fluid imprint and inertial switching in ferroelectric La: HfO_2 capacitors, ACS Appl. Mater. Interfaces **11**, 35115 (2019).

[12] M. H. Park, Y. H. Lee, H. J. Kim, Y. J. Kim, T. Moon, K. D. Kim, J. Müller, A. Kersch, U. Schroeder, T. Mikolajick, and C. S. Hwang, Ferroelectricity and antiferroelectricity of doped thin HfO_2-based films, Adv. Mater. **27**, 1811 (2015).

[13] T. D. Huan, V. Sharma, G. A. Rossetti, and R. Ramprasad, Pathways towards ferroelectricity in Hafnia, Phys. Rev. B **90**, 064111 (2014).

[14] S. E. Reyes-Lillo, K. F. Garrity, and K. M. Rabe, Antiferroelectricity in thin-film ZrO_2 from first principles, Phys. Rev. B **90**, 140103(R) (2014).

[15] X. Sang, E. D. Grimley, T. Schenk, U. Schroeder, and J. M. LeBeau, On the structural origins of ferroelectricity in HfO_2 thin films, Appl. Phys. Lett. **106**, 162905 (2015).

[16] R. Materlik, C. Künneth, and A. Kersch, The origin of ferroelectricity in $Hf_{1-x}Zr_xO_2$: A computational investigation and a surface energy model, J. Appl. Phys. **117**, 134109 (2015).

[17] P. Polakowski and J. Müller, Ferroelectricity in undoped hafnium oxide, Appl. Phys. Lett. **106**, 232905 (2015).

[18] R. Batra, H. D. Tran, and R. Ramprasad, Stabilization of metastable phases in hafnia owing to surface energy effects, Appl. Phys. Lett. **108**, 172902 (2016).

[19] C. Künneth, R. Materlik, and A. Kersch, Modeling ferroelectric film properties and size effects from tetragonal interlayer in $Hf_{1-x}Zr_xO_2$ grains, J. Appl. Phys. **121**, 205304 (2017).

[20] M. H. Park, Y. H. Lee, H. J. Kim, T. Schenk, W. Lee, K. D. Kim, F. P. G. Fengler, T. Mikolajick, U. Schroeder, and C. S. Hwang, Surface and grain boundary energy as the key enabler of ferroelectricity in nanoscale hafnia-zirconia: A comparison of model and experiment, Nanoscale **9**, 9973 (2017).

[21] T. Shiraishi, K. Katayama, T. Yokouchi, T. Shimizu, T. Oikawa, O. Sakata, H. Uchida, Y. Imai, T. Kiguchi, T. J. Konno, and H. Funakubo, Impact of mechanical stress on ferroelectricity in $Hf_{0.5}Zr_{0.5}O_2$ thin films, Appl. Phys. Lett. **108**, 262904 (2016).

[22] R. Batra, T. D. Huan, J. L. Jones, G. Rossetti, and R. Ramprasad, Factors favoring ferroelectricity in Hafnia: A first-principles computational study, J. Phys. Chem. C **121**, 4139 (2017).

[23] S. Liu and B. M. Hanrahan, Effects of growth orientations and epitaxial strains on phase stability of HfO_2 thin films, Phys. Rev. Mater. **3**, 054404 (2019).

[24] U. Schroeder, E. Yurchuk, J. Müller, D. Martin, T. Schenk, P. Polakowski, C. Adelmann, M. I. Popovici, S. V. Kalinin, and T. Mikolajick, Impact of different dopants on the switching properties of ferroelectric hafnium oxide, Jpn. J. Appl. Phys. **53**, 08LE02 (2014).

[25] S. Starschich and U. Boettger, An extensive study of the influence of dopants on the ferroelectric properties of HfO_2, J. Mater. Chem. C **5**, 333 (2017).

[26] M. H. Park, T. Schenk, C. M. Fancher, E. D. Grimley, C. Zhou, C. Richter, J. M. LeBeau, J. L. Jones, T. Mikolajick, and U. Schroeder, A comprehensive study on the structural evolution of HfO_2 thin films doped with various dopants, J. Mater. Chem. C **5**, 4677 (2017).

[27] L. Xu, T. Nishimura, S. Shibayama, T. Yajima, S. Migita, and A. Toriumi, Kinetic pathway of the ferroelectric phase formation in doped HfO_2 films, J. Appl. Phys. **122**, 124104 (2017).

[28] R. Batra, T. D. Huan, G. A. Rossetti, and R. Ramprasad, Dopants promoting ferroelectricity in Hafnia: Insights from a comprehensive chemical space exploration, Chem. Mater. **29**, 9102 (2017).

[29] L. Xu, T. Nishimura, S. Shibayama, T. Yajima, S. Migita, and A. Toriumi, Ferroelectric phase stabilization of HfO_2 by nitrogen doping, Appl. Phys. Express **9**, 091501 (2016).

[30] A. Pal, V. K. Narasimhan, S. Weeks, K. Littau, D. Pramanik, and T. Chiang, Enhancing ferroelectricity in dopant-free hafnium oxide, Appl. Phys. Lett. **110**, 022903 (2017).

[31] E. D. Grimley, T. Schenk, T. Mikolajick, U. Schroeder, and J. M. LeBeau, Atomic structure of domain and interphase boundaries in ferroelectric HfO_2, ACS Appl. Mater. Interfaces **5**, 1701258 (2018).

[32] C. Richter, T. Schenk, M. H. Park, F. A. Tscharntke, E. D. Grimley, J. M. LeBeau, C. Zhou, C. M. Fancher, J. L. Jones, T. Mikolajick, and U. Schroeder, Si doped hafnium oxide—A "fragile" ferroelectric system, Adv. Electron. Mater. **3**, 1700131 (2017).

[33] A. Chouprik, D. Negrov, E. Y. Tsymbal, and A. Zenkevich, Defects in ferroelectric HfO_2, Nanoscale **13**, 11635 (2021).

[34] Y. Qi, S. Singh, and K. M. Rabe, Polarization switching mechanism in HfO_2 from first-principles lattice mode analysis, arXiv:2108.12538.

[35] VASP the guide, https://www.vasp.at/wiki/index.php/The_VASP_Manual, 2022.

[36] V. F. Michel, T. Esswein, and N. A. Spaldin, Interplay between ferroelectricity and metallicity in $BaTiO_3$, J. Mater. Chem. C **9**, 8640 (2021).

[37] F. Delodovici, P. Barone, and S. Picozzi, Trilinear-coupling-driven ferroelectricity in HfO_2, Phys. Rev. Mater. **5**, 064405 (2021).

[38] S. Guha and V. Narayanan, OxygenVacancies in High Dielectric Constant Oxide-Semiconductor Films, Phys. Rev. Lett. **98**, 196101 (2007).

[39] E. Cho, B. Lee, C.-K. Lee, S. Han, S. H. Jeon, B. H. Park, and Y.-S. Kim, Segregation of oxygen vacancy at metal-HfO_2 interfaces, Appl. Phys. Lett. **92**, 233118 (2008).

[40] W. Hamouda, C. Lubin, S. Ueda, Y. Yamashita, O. Renault, F. Mehmood, T. Mikolajick, U. Schroeder, R. Negrea, and N. Barrett, Interface chemistry of pristine TiN/La: $Hf_{0.5}Zr_{0.5}O_2$ capacitors, Appl. Phys. Lett. **116**, 252903 (2020).

[41] F. P. G. Fengler, R. Nigon, P. Muralt, E. D. Grimley, X. Sang, V. Sessi, R. Hentschel, J. M. LeBeau, T. Mikolajick, and U. Schroeder, Analysis of performance instabilities of hafnia-based ferroelectrics using modulus spectroscopy and thermally stimulated depolarization currents, Adv. Electron. Mater. **4**, 1700547 (2018).

[42] K. Z. Rushchanskii, S. Blügel, and M. Ležaić, Ordering of Oxygen Vacancies and Related Ferroelectric Properties in $HfO_{2-\delta}$, Phys. Rev. Lett. **127**, 087602 (2021).

[43] J. P. Perdew, K. Burke, and M. Ernzerhof, Generalized Gradient Approximation Made Simple, Phys. Rev. Lett. **77**, 3865 (1996).

[44] A. R. Oganov and C. W. Glass, Crystal structure prediction using ab initio evolutionary techniques: Principles and applications, J. Chem. Phys. **124**, 244704 (2006).

[45] A. O. Lyakhov, A. R. Oganov, H. T. Stokes, and Q. Zhu, New developments in evolutionary structure prediction algorithm USPEX, Comput. Phys. Commun. **184**, 1172 (2013).

[46] A. R. Oganov, A. O. Lyakhov, and M. Valle, How evolutionary crystal structure prediction works—And why, Acc. Chem. Res. **44**, 227 (2011).

[47] J. Sun, A. Ruzsinszky, and J. P. Perdew, Strongly Constrained and Appropriately Normed Semilocal Density Functional, Phys. Rev. Lett. **115**, 036402 (2015).

[48] See Supplemental Material at http://link.aps.org/supplemental/10.1103/PhysRevLett.130.096801 for results of additional calculations, which includes Refs. [11,23, 49–68].

[49] I. MacLaren, T. Ras, M. MacKenzie, A. J. Craven, D. W. McComb, and S. D. Gendt, Texture, twinning, and metastable "tetragonal" phase in ultrathin films of HfO_2 on a Si substrate, J. Electrochem. Soc. **156**, G103 (2009).

[50] M. Hoffmann, U. Schroeder, T. Schenk, T. Shimizu, H. Funakubo, O. Sakata, D. Pohl, M. Drescher, C. Adelmann, R. Materlik, A. Kersch, and T. Mikolajick, Stabilizing the ferroelectric phase in doped hafnium oxide, J. Appl. Phys. **118**, 072006 (2015).

[51] J. Wu, Impact of oxygen vacancies on monoclinic hafnium oxide and band alignment with semiconductors, Mater. Today Commun. **25**, 101482 (2020).

[52] R.-C. Fang, Q.-Q. Sun, P. Zhou, W. Yang, P.-F. Wang, and D. W. Zhang, High-performance bilayer flexible resistive random access memory based on low-temperature thermal atomic layer deposition, Nanoscale Res. Lett. **8**, 92 (2013).

[53] C. Quinteros, R. Zazpe, F. G. Marlasca, F. Golmar, F. Casanova, P. Stoliar, L. Hueso, and P. Levy, HfO_2 based memory devices with rectifying capabilities, J. Appl. Phys. **115**, 024501 (2014).

[54] D. Duncan, B. Magyari-Kope, and Y. Nishi, Filament-induced anisotropic oxygen vacancy diffusion and charge trapping effects in hafnium oxide RRAM, IEEE Electron Device Lett. **37**, 400 (2016).

[55] Y. Hou, U. Celano, L. Goux, L. Liu, A. Fantini, R. Degraeve, A. Youssef, Z. Xu, Y. Cheng, J. Kang, M. Jurczak, and W. Vandervorst, Sub-10 nm low current resistive switching behavior in hafnium oxide stack, Appl. Phys. Lett. **108**, 123106 (2016).

[56] A. K. Singh, S. Blonkowski, and M. Kogelschatz, Resistive switching study in HfO_2 based resistive memories by conductive atomic force microscopy in vacuum, J. Appl. Phys. **124**, 014501 (2018).

[57] V. Antad, P. A. Shaikh, A. Biswas, S. S. Rajput, S. Deo, M. V. Shelke, S. Patil, and S. Ogale, Resistive switching in $HfO_{2-x}/La_{0.67}Sr_{0.33}MnO_3$ heterostructures: An intriguing case of low H-field susceptibility of an E-field controlled active interface, ACS Appl. Mater. Interfaces **13**, 54133 (2021).

[58] S. Clima, Y. Y. Chen, R. Degraeve, M. Mees, K. Sankaran, B. Govoreanu, M. Jurczak, S. D. Gendt, and G. Pourtois, First-principles simulation of oxygen diffusion in HfO_x: Role in the resistive switching mechanism, Appl. Phys. Lett. **100**, 133102 (2012).

[59] K. Kamiya, M. Y. Yang, T. Nagata, S.-G. Park, B. Magyari-Köpe, T. Chikyow, K. Yamada, M. Niwa, Y. Nishi, and K. Shiraishi, Generalized mechanism of the resistance switching in binary-oxide-based resistive random-access memories, Phys. Rev. B **87**, 155201 (2013).

[60] S. Dirkmann, J. Kaiser, C. Wenger, and T. Mussenbrock, Filament growth and resistive switching in hafnium oxide memristive devices, ACS Appl. Mater. Interfaces **10**, 14857 (2018).

[61] D.-H. Kwon, K. M. Kim, J. H. Jang, J. M. Jeon, M. H. Lee, G. H. Kim, X.-S. Li, G.-S. Park, B. Lee, S. Han, M. Kim, and C. S. Hwang, Atomic structure of conducting nanofilaments in TiO_2 resistive switching memory, Nat. Nanotechnol. **5**, 148 (2010).

[62] S. Kang, W.-S. Jang, A. N. Morozovska, O. Kwon, Y. Jin, Y.-H. Kim, H. Bae, C. Wang, S.-H. Yang, A. Belianinov *et al.*, Highly enhanced ferroelectricity in HfO_2-based ferroelectric thin film by light ion bombardment, Science **376**, 731 (2022).

[63] R. Zhang, H. Huang, Q. Xia, C. Ye, X. Wei, J. Wang, L. Zhang, and L. Q. Zhu, Role of oxygen vacancies at the TiO_2/HfO_2 interface in flexible oxide-based resistive switching memory, Adv. Electron. Mater. **5**, 1800833 (2019).

[64] E. D. Grimley, T. Schenk, X. Sang, M. Pešić, U. Schroeder, T. Mikolajick, and J. M. LeBeau, Structural changes underlying field-cycling phenomena in ferroelectric HfO_2 thin films, Adv. Electron. Mater. **2**, 1600173 (2016).

[65] T. Mittmann, M. Materano, S.-C. Chang, I. Karpov, T. Mikolajick, and U. Schroeder, Impact of oxygen vacancy content in ferroelectric HZO films on the device performance, *2020 IEEE International Electron Devices Meeting (IEDM)* (IEEE, New York, 2020), p. 18.4.1, 10.1109/iedm13553.2020.9372097.

[66] Z. Fan, J. Deng, J. Wang, Z. Liu, P. Yang, J. Xiao, X. Yan, Z. Dong, J. Wang, and J. Chen, Ferroelectricity emerging in strained (111)-textured ZrO_2 thin films, Appl. Phys. Lett. **108**, 012906 (2016).

[67] R. He, H. Wu, S. Liu, H. Liu, and Z. Zhong, Ferroelectric structural transition in hafnium oxide induced by charged oxygen vacancies, Phys. Rev. B **104**, L180102 (2021).

[68] P. Nukala, M. Ahmadi, Y. Wei, S. de Graaf, E. Stylianidis, T. Chakrabortty, S. Matzen, H. W. Zandbergen, A. Björling, D. Mannix, D. Carbone, B. Kooi, and B. Noheda, Reversible oxygen migration and phase transitions in hafnia-based ferroelectric devices, Science **372**, 630 (2021).

[69] Y. Wei, P. Nukala, M. Salverda, S. Matzen, H. J. Zhao, J. Momand, A. S. Everhardt, G. Agnus, G. R. Blake, P. Lecoeur, B. J. Kooi, J. Íñiguez, B. Dkhil, and B. Noheda, A rhombohedral ferroelectric phase in epitaxially strained $Hf_{0.5}Zr_{0.5}O_2$ thin films, Nat. Mater. **17**, 1095–1100 (2018).

[70] Y. Qi, S. Singh, C. Lau, F.-T. Huang, X. Xu, F. J. Walker, C. H. Ahn, S.-W. Cheong, and K. M. Rabe, Stabilization of Competing Ferroelectric Phases of HfO_2 Under Epitaxial Strain, Phys. Rev. Lett. **125**, 257603 (2020).

[71] L. Baumgarten, T. Szyjka, T. Mittmann, M. Materano, Y. Matveyev, C. Schlueter, T. Mikolajick, U. Schroeder, and M. Müller, Impact of vacancies and impurities on ferroelectricity in PVD- and ALD-grown HfO_2 films, Appl. Phys. Lett. **118**, 032903 (2021).

[72] T. Mittmann, M. Materano, P. D. Lomenzo, M. H. Park, I. Stolichnov, M. Cavalieri, C. Zhou, C.-C. Chung, J. L. Jones, T. Szyjka, M. Müller, A. Kersch, T. Mikolajick, and U. Schroeder, Origin of ferroelectric phase in undoped HfO_2 films deposited by sputtering, Adv. Mater. Interfaces **6**, 1901528 (2019).

[73] Y. Zhou, Y. Zhang, Q. Yang, J. Jiang, P. Fan, M. Liao, and Y. Zhou, The effects of oxygen vacancies on ferroelectric phase transition of HfO_2-based thin film from first-principle, Comput. Mater. Sci. **167**, 143 (2019).

[74] S. J. Kim, D. Narayan, J.-G. Lee, J. Mohan, J. S. Lee, J. Lee, H. S. Kim, Y.-C. Byun, A. T. Lucero, C. D. Young, S. R. Summerfelt, T. San, L. Colombo, and J. Kim, Large ferroelectric polarization of $TiN/Hf_{0.5}Zr_{0.5}O_2/TiN$ capacitors due to stress-induced crystallization at low thermal budget, Appl. Phys. Lett. **111**, 242901 (2017).

[75] J. Wan, X. Chen, L. Ji, Z. Tu, H. Wu, and C. Liu, Ferroelectricity of $Hf_{0.5}Zr_{0.5}O_2$ thin films free from the influence of electrodes by using Al_2O_3 capping layers, IEEE Trans. Electron Devices **69**, 1805 (2022).

[76] J. Robertson, O. Sharia, and A. A. Demkov, Fermi level pinning by defects in HfO_2-metal gate stacks, Appl. Phys. Lett. **91**, 132912 (2007).

[77] Y. Yun, P. Buragohain, M. Li, Z. Ahmadi, Y. Zhang, X. Li, H. Wang, J. Li, P. Lu, L. Tao, H. Wang, J. E. Shield, E. Y. Tsymbal, A. Gruverman, and X. Xu, Intrinsic ferroelectricity in Y-doped HfO_2 thin films, Nat. Mater. **21**, 903 (2022).

[78] N. Umezawa, K. Shiraishi, T. Ohno, H. Watanabe, T. Chikyow, K. Torii, K. Yamabe, K. Yamada, H. Kitajima, and T. Arikado, First-principles studies of the intrinsic effect of nitrogen atoms on reduction in gate leakage current through Hf-based high-k dielectrics, Appl. Phys. Lett. **86**, 143507 (2005).

[79] H. Wang, F. Tang, M. Stengel, H. Xiang, Q. An, T. Low, and X. Wu, Convert Widespread Paraelectric Perovskite to Ferroelectrics, Phys. Rev. Lett. **128**, 197601 (2022).

[80] J. Wei, L. Jiang, M. Huang, Y. Wu, and S. Chen, Intrinsic defect limit to the growth of orthorhombic HfO_2 and $(Hf,Zr)O_2$ with strong ferroelectricity: First-principles insights, Adv. Funct. Mater. **31**, 2104913 (2021).